ELSEVIER

Journal of Photochemistry and Photobiology A: Chemistry 97 (1996) 73–79

Journal of PHOTOCHEMISTRY AND PHOTOBIOLOGY A:CHEMISTRY

The mechanism of the photoreaction of uranyl 1,3-diketonate complexes as thin films on silicon surfaces

M. Gao, Ross H. Hill *

Department of Chemistry, Simon Fraser University, Burnaby, B.C. V5A 1S6, Canada

Received 27 October 1995; accepted 9 January 1996

Abstract

The photolysis of the complexes $UO_2(OH_2)(RCOCHCOR)_2$ (R = Me or t-C_4H_9) on silicon surfaces leads to the production of uranium oxide. The quantum yields for this process are quite different for the two complexes. The methyl and the *tert*-butyl-substituted complexes decompose with quantum yields of 0.007 (±40%) and 0.015 (±30%) respectively. In spite of the similarity in chemical formula a detailed mechanistic investigation indicates that two distinct reaction pathways exist for these systems. In the case of the methyl derivative the reactivity is initiated by an excited state hydrogen abstraction through a six-member transition state. The *tert*-butyl-substituted complex cannot undergo hydrogen abstraction and so the excited state decays by a ligand fragmentation reaction.

Keywords: Photoreaction; Uranyl 1,3-diketonate; Thin films; Silicon surfaces

1. Introduction

We wish to report the varied mechanisms of the photochemistry of uranyl 1,3-diketonate complexes in thin amorphous films. Our interest in these compounds is part of a program aimed at the development of the solid state photochemistry of thin amorphous films [1]. Our efforts have led to the development of the photochemistry of systems which may be used in lithographic processes to deposit materials such as metals [2–8] and metal oxides [3,9,10]. These materials have obvious practical importance in the microelectronics field. As part of this study we initiated an investigation of possible routes to deposit uranium-containing films [3,11]. Thin films of uranium, or its oxides, may be useful for the construction of the opaque regions of an X-ray mask [12]. The high absorption cross-section of uranium makes it ideal for use in such an application [13].

Previously we reported the production of uranium oxide upon photolysis of thin films of a variety of uranyl complexes [3, 11]. Metal 1,3-diketonates have been used for chemical vapor deposition in the past [14] and the solution chemistry has been extensively studied [15]. Of importance here is our previous study of the two complexes with diketonate ligands, $UO_2(OH_2)(RCOCHCOR)_2$ (R = Me (acac) or t-C_4H_9 (t-Bu-acac)). Thin films of either of these on silicon surfaces yielded pure films of amorphous uranium oxide. The initial work showed that $UO_2(OH_2)(acac)_2$ was unable to form sufficiently thin films to be of practical use [11]. We hence prepared and studied the *tert*-butyl derivative with the expectation that the larger organic groups would lower the intermolecular forces, allowing us to prepare thicker amorphous films. While this expectation was confirmed [3], qualitative observations suggested that the latter complex underwent more efficient photochemistry. To provide some fundamental information regarding both the efficiency and the details of the photoreactivity we undertook a mechanistic study of the photoreactions of these systems.

2. Experimental section

All silicon wafers were obtained from Shin Etsu and were p-type Si(100). The wafers were cut to the approximate dimensions of 1 cm × 1.5 cm in house. The NaCl and CaF_2 crystals were obtained from Wilmad Glass Co. Inc. Both complexes were prepared by literature procedures [16] and characterized by their elemental analysis and Fourier transform IR (FTIR) spectra.

FTIR spectra were obtained with a Bomem MB-120 on samples held in an aluminum vacuum chamber equipped with NaCl optics by steel clips. The film thickness was determined using a Leitz Laborlux 12 ME S with an interference attach-

* Corresponding author.

PII S1010-6030(96)04312-2

ment [17]. The irradiation source was either a 100 W high pressure Hg lamp in an Oriel housing equipped with condenser lenses and filtered through a 10 cm water filter with quartz optics or an Oriel 254 nm monochromatic pencil-type low pressure Hg lamp equipped with a 6047 a.c. power supply. The intensity of the light source was measured with an International Light IL 1350 radiometer and the output was found to be constant (within error 10%) by periodic measurement of intensity throughout the experiments.

2.1. Preparation of the amorphous thin films

The thin films of the precursor complexes were prepared from solutions of the complexes in CH_2Cl_2. A silicon chip was placed on a Laurell Technology Corporation spin coater and rotated at a speed of 1000 rev min^{-1}. A portion (0.5 ml) of a solution of the uranyl diketonate complex in CH_2Cl_2 was dispensed onto the silicon chip and allowed to spread. The motor was then stopped and a thin film of the complex remained on the chip.

2.2. Calibration of the Fourier transform IR and UV–visible absorption on silicon surfaces

A solution of $UO_2(OH_2)$(*t*-Bu–acac)$_2$ in CH_2Cl_2 (0.0058 g in 3.0 ml) was prepared. A drop (0.0025 ml) of this solution was placed on the silicon surface and allowed to dry. The area of the dried drop was 0.22 cm^2 and corresponded to a coverage of 2 molecules A^{-2}. The FTIR data of the surface were obtained. This process was repeated several times and the spectra collected with each additional drop (Fig. 1(a)). A plot of the absorbance at 1351 cm^{-1} vs. coverage was linear as shown in Fig. 1(b)). The slope of this plot yielded an extinction coefficient of 4.4×10^3 A^2 molecule^{-1}. The spectral data are reported later in Table 1 for all other peaks.

The extinction coefficients for the UV–visible data were determined in the following way. A film of $UO_2(OH_2)$(*t*-Bu–acac)$_2$ was cast from CH_2Cl_2 onto a CaF_2 surface by spin coating. Both the UV–visible and FTIR spectra were obtained for this surface. The extinction coefficients for the UV–visible data were obtained relative to the above determined FTIR bands and are reported later in Table 1.

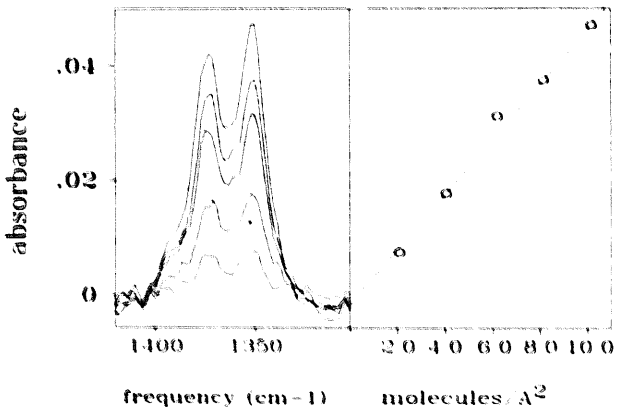

Fig. 1. (Left) FTIR spectra of a film composed of 2.0, 4.0, 6.0, 8.0 and 10.0 molecules $Å^{-2}$ of $UO_2(OH_2)$(*t*-Bu–acac)$_2$ on a Si surface. (Right) Plot of the absorbance of 1351 cm^{-1} band of $UO_2(OH_2)$(*t*-Bu–acac)$_2$ vs. coverage.

A similar experiment with $UO_2(OH_2)(acac)_2$ has been reported previously and yielded an extinction coefficient of 3.3×10^3 A^2 molecule^{-1} at 1524 cm^{-1}. The UV–visible data were obtained as above and all the data, FTIR and UV–visible, are presented later in Table 1 and Table 2.

2.3. Photolysis of complexes as films on silicon surfaces; quantum yield determination

A typical quantum yield experiment performed in the air is described below. A Si chip with a $UO_2(OH_2)$(*t*-Bu–acac)$_2$ film was placed on a brass sample holder. The low pressure Hg lamp (254 nm) was then placed 1.5 cm from the film. The FTIR spectrum of the starting film was first obtained. The film was then irradiated for 35 min and the FTIR spectrum obtained again. The same procedure was followed and FTIR spectra were recorded for each subsequent irradiation period of 70, 130, 255, 420, 740 and 1360 min. A record of the absorbance of the band at 1351 cm^{-1} vs. photolysis time was made. A plot of A_t vs. photolysis time was fitted to a single-exponential decay in order to get the decay constant for the quantum yield calculation.

$$\ln\left(\frac{A_0}{A_t}\right) = (2.303 I \Phi \epsilon_\lambda) t \qquad (1)$$

The quantum yield for loss of the metal complex ML_n can be calculated from Eq. 1 [6]. The derivation of this equation is only valid when the film absorbance, at the excitation wavelength, is small. In this equation, I represents the incident light intensity, and ϵ_λ the extinction coefficient of the metal complex at the irradiation wavelength (in units of square centimeter per mole). The exponential form was used for fitting in order to prevent weighting of the experimental points by the logarithm function.

The initial absorbances at the irradiation wavelengths were 0.2 and 0.264 for the *tert*-butyl and methyl derivatives respectively. This corresponds to introducing an error of 25% and 35% into the light absorption early in the reaction and contributes to the large estimated error in the quantum yields.

2.4. Mass spectrometry analyses of volatile products

A silicon chip (1.0 cm × 2.5 cm) coated with a film of $UO_2(OH_2)$(*t*-Bu–acac)$_2$ was placed in a quartz vacuum sample tube. The system was evacuated to a vacuum of approximately 10^{-3} Torr and closed. The sample was then irradiated with 254 nm UV light for 10 h. The volatile products generated from the photolysis of $UO_2(OH_2)$(*t*-Bu–acac)$_2$ remained in the system ready for the mass spectrometry (MS) analysis.

The mass spectra were recorded with an HP 5958 gas chromatography–MS spectrometer. An electron-impact ion source was used and the ion source temperature was 200 °C.

The resolution was 1000 amu^{-1}. The electron energy for ionization was 70 eV. About 200 mass spectra were recorded for rebuilding a total ion current (TIC) spectrum. The scanning mass range was 20–300 amu.

Similar experiments were conducted with $UO_2(OH_2)(acac)_2$.

3. Results

3.1. Spectroscopy

The FTIR spectral data for both uranyl 1,3-diketonate complexes are in Table 1. Both thin film data and the literature data [16,18] for microcrystalline samples are found in this table and are comparable. The extinction coefficients and assignments [18–21] are also included in the table. Since we use the absorbance to monitor the extent reaction for the quantum yields, it is important to establish that thin films of these complexes exhibit Beer–Lambert behavior. In Fig. 1 a plot of a region of the FTIR spectra of $UO_2(OH_2)(t\text{-Bu-acac})_2$ as a film deposited on a silicon wafer is shown. Accompanying this figure is a plot of absorbance vs. coverage which is linear and establishes that absorbance on the surface can be used to monitor extent reaction.

UV–visible spectroscopy was also used to characterize $UO_2(OH_2)(t\text{-Bu-acac})_2$ and $UO_2(OH_2)(acac)_2$. The UV–visible spectra of $UO_2(OH_2)(acac)_2$ had absorption bands in the region of 290 and 370 nm (Table 2). The absorption band at 290 nm is assigned to intraligand π–π^* transition [15]. The shape of this band is asymmetric, indicating that there might be a ligand-to-metal charge transfer band obscured on the higher energy side. A band in the region of 370 nm is associated with the uranyl group [22]. For quantitative work the quantum yield was measured using 254 nm light associated with high energy ligand-to-metal charge transfer transitions.

Table 1
FTIR spectral data for the uranyl complexes

Complex	FTIR, ν (cm^{-1}) ($\log \epsilon$ (mol $cm\,l^{-1}$))		Assignment
	Crystalline state	Film	
$UO_2(OH_2)(acac)_2$	1570	1574 (2.24)	ν_s(CO)
	1529	1524 (2.30)	ν_{as}(CC)
	1437	1429 (1.73)	ν(CH)
	1351	1362 (2.18)	ν_{as}(CO)
	1227	1271 (1.80)	ν_s(CC)
	1024, 1014	1015 (1.63)	ν(CH_3)
	925	920 (2.11)	ν_{as}(UO)
$UO_2(OH_2)(t\text{-Bu-acac})_2$	1565, 1545	1564, 1547 (2.46, 2.53)	ν_s(CO)
	1534	1537 (2.08)	ν_{as}(CCC)
	1500	1503 (2.46)	ν_{as}(CO)
	1372, 1350	1374, 1351 (2.37, 2.42)	δ(CH_3)
	1246	1247 (1.78)	ν_s(CCC)
	1224	1226 (1.94)	ρ(CH_3)
	1145	1146 (2.08)	δ(CH_3)
	892	887 (2.28)	ν_{as}(UO)

Table 2
UV–visible spectral data of the uranyl complexes

Complex	UV–visible, λ_{max} (nm) ($\log \epsilon$ (mol $cm\,l^{-1}$))	
	Film	Solution [a]
$UO_2(OH_2)(acac)_2$	290 (3.34)	273
	365 (2.59)	347
$UO_2(OH_2)(t\text{-Bu-acac})_2$	290 (3.48)	
	370 (2.85)	

[a] From [16].

Table 3
Auger electron spectroscopy analysis of the photoproduced films

Film precursor	I_0/I_U	Composition
UO_3 standard	3.9 (±0.6)	UO_3
$UO_2(OH_2)(acac)_2$	3.9 (±0.6)	$UO_{3(\pm 0.9)}$
$UO_2(OH_2)(t\text{-Bu-acac})_2$	4.5 (±0.6)	$UO_{3.5(\pm 0.9)}$

Table 4
Mass spectral data

Complex	m/z	Assignment
$UO_2(OH_2)(acac)_2$	100, 85, 43	MeCOCHCOMeH
	100, 71, 57, 43	$CH_2C(O)C(OH)(CH_3)CH_2$
$UO_2(OH_2)(t\text{-Bu-acac})_2$	184, 127, 109, 85, 81, 69, 57, 43, 41	t-BuCOCHCOt-BuH
	114, 109, 57	$(CH_3)_3CC(CH_3)_3$
	100, 85, 57, 43	$CH_3C(O)(CH_3)_3$
	86, 85, 71, 57, 43	$(CH_3)_3CC(O)H$
	84, 69, 43, 41	$CH_2C(CH_3)C(O)CH_3$

The energy of the transitions observed in thin films are shifted 18 nm to lower energy compared with the result in ethanol solution reported by Comyns et al. [16]. This presumably results from the interaction between polar solvent and sample molecules. It is known that a polar solvent usually increases the energies of π–π^* transitions [22]. In films, there is no solvent–sample interaction; so the absorption energies that we obtained from films appeared to lower energies.

The UV–visible spectrum of the $UO_2(OH_2)(t\text{-Bu-acac})_2$ thin film was very similar to the spectrum of $UO_2(OH_2)(acac)_2$. The absorption bands and the extinction coefficients are listed in Table 2.

3.2. Characterization of the reaction products

3.2.1. Solid phase products

The photolysis of thin films of either of the 1,3 diketonate complexes results in the loss of the absorption bands associated with the complexes. The final films show absorption bands in the region of 900 cm^{-1}. These bands are associated

with the retention of the oxygen, indicating the formation of uranium oxides [23]. This interpretation is also substantiated by Auger electron spectroscopy which has been used to measure the stoichiometry of the retained oxide. In Table 3 the Auger electron data are presented. The data were based upon the intensity of the oxygen signal near 500 eV and the uranium signal at 78 eV. By utilizing a commercially obtained UO_3 standard the stoichiometry was established as within error of UO_3 for all the materials produced in this study.

3.2.2. *Mass spectral analysis of the volatile products*

Since the organic products of the surface reactions were not evident on the surface, it was apparent that the fragments could be found in the gas phase. In order to identify these products surfaces were photolysed and the gaseous fragments monitored by mass spectral analysis. In Table 4 the fragments detected are listed together with the observed mass and assignments.

Only two volatile organic products were detected following the photolysis of $UO_2(OH_2)(acac)_2$. The first was simply the free ligand, $MeCOCH_2COMe$, while the second was an isomerization product of this ligand, 3-hydroxyl,3-methyl cyclobutanone. A more complicated set of products was observed over the $UO_2(OH_2)(t\text{-Bu-acac})_2$ film.

Photolysis of a surface film of $UO_2(OH_2)(t\text{-Bu-acac})_2$ yielded the free ligand, t-$BuCOCH_2COt$-Bu, and a variety of fragmentation products. These fragmentation products, listed in Table 4, will be discussed in Section 4.2.

3.3. *Quantum yield determinations*

The quantum yields for the previously reported decomposition reactions of the two 1,3 diketonate complexes were also measured. Thin films of $UO_2(OH_2)(t\text{-Bu-acac})_2$ were prepared and photolysed with monochromatic light at 254 nm. The FTIR spectral changes associated with the photolysis of a 580 monolayer film of $UO_2(OH_2)(t\text{-Bu-acac})_2$ are illustrated in Fig. 2. The photolysis of $UO_2(OH_2)(t\text{-Bu-acac})_2$ led to the loss of all the FTIR bands associated with diketonate ligand at 1564, 1547, 1503, 1374, 1351, 1226 and 1146 cm^{-1}.

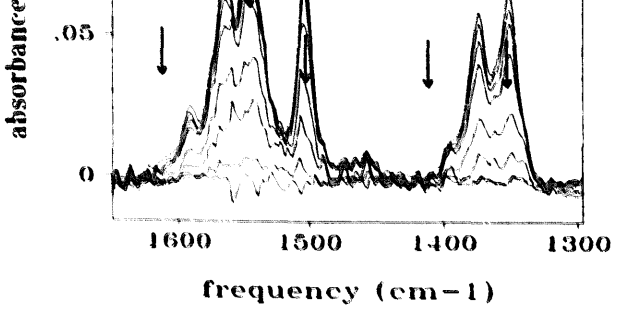

Fig. 2. Changes in FTIR spectra of $UO_2(OH_2)(t\text{-Bu-acac})_2$ thin film upon photolysis for 0, 35, 70, 130, 255, 420, 740 and 1360 min with 254 nm light.

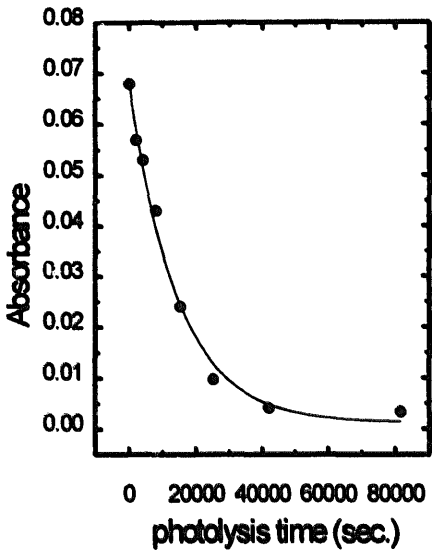

Fig. 3. Plot showing the absorbance A_t at 1351 cm^{-1} vs. photolysis time in the photolysis of $UO_2(OH_2)(t\text{-Bu-acac})_2$ with 254 nm light.

The asymmetric stretching band of O=U=O at 887 cm^{-1} (not shown) decreased and concomitant growth of a band at 904 cm^{-1} (not shown) indicated the formation of the UO_3 film. There was no detectable intermediate observed during the photolysis.

The decomposition quantum yield of $UO_2(OH_2)(t\text{-Bu-acac})_2$ was determined on the basis of FTIR spectroscopy data of the photolysis experiment. The IR absorbance A_0 of the starting material at 1351 cm^{-1} and the absorbance A_t of this band as a function of photolysis time were measured. A plot of A_t vs. photolysis time (Fig. 3) was then made. This plot is fitted to an exponential decay and is consistent with a single-photon process. The quantum yield was determined by the decay constant of the plot, the intensity of the irradiation light and the extinction coefficient of absorption at the irradiation wavelength according to Eq. (1). The quantum yield was 0.015 (±30%).

A similar photolysis experiment was conducted with $UO_2(OH_2)(acac)_2$. The photolysis of thin films of $UO_2(OH_2)(acac)_2$ resulted in the loss of all IR absorption bands associated with the acetylacetonate ligand at 1574, 1524, 1429, 1362, 1271 and 1015 cm^{-1}. The loss of the asymmetric stretching band of O=U=O at 916 cm^{-1} was accompanied by the appearance of a band at 908 cm^{-1} associated with the asymmetric stretching of UO_3.

The plot of A_t for the absorption at 1524 cm^{-1} vs. photolysis fitted a single-exponential decay. The disappearance quantum yield of $UO_2(OH_2)(acac)_2$ was found to be 0.007 (±40%).

$UO_2(OH_2)(t\text{-Bu-acac})_2$ reacted with a higher quantum yield than $UO_2(OH_2)(acac)_2$. This is attributed to the bulky ligand in the $UO_2(OH_2)(t\text{-BuCOCHCO}t\text{-Bu})_2$ molecule. The bulky ligand, t-$BuCOCHCOt$-Bu, creates spaces between molecules in the film to allow the photochemically produced fragments to eject from the surface.

4. Discussion

The photolysis of both $UO_2(OH_2)(acac)_2$ and $UO_2(OH_2)(t\text{-Bu–acac})_2$ are single photon processes:

$$UO_2(OH_2)L_2 \xrightarrow{h\nu} UO_3 + \text{organic products} \quad (2)$$

where L = acac or *t*-Bu–acac.

We will examine the detailed mechanism of each of these reactions in the following sections.

4.1. Mechanism of the photolysis of $UO_2(OH_2)(acac)_2$

Both FTIR spectral data and Auger photoelectron spectroscopy are indicative of the production of UO_3. The single-exponential decay of A_t vs. photolysis time is consistent with there being no thermally stable intermediates formed in the reaction. The organic products are derived from the ligands. The overall reaction is

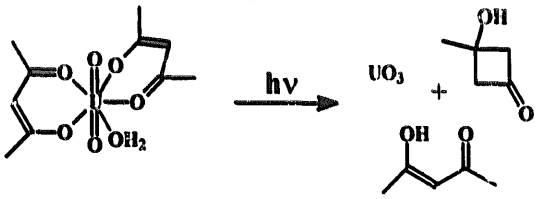

(3)

It is important to note that the stoichiometry shown in Eq. (3) has not been unequivocally established. The intensity of the mass spectral signals are not indicative of the relative amounts of these materials formed. In spite of this the stoichiometry listed is consistent with what appears to be the most reasonable mechanism which is outlined in Scheme 1.

The reaction is initiated by the absorption of a photon which results in a ligand-to-metal charge transfer transition in the starting material, $UO_2(OH_2)(acac)_2$. The effect of this transition is to cleave a uranium oxygen bond. The abstraction of a γ-hydrogen atom from the remote methyl group by the oxygen atom with the unpaired electron occurs through a six-member transition state. This transfer initiates the cyclization shown in the scheme [24]. This product then releases the cyclized ligand following a hydrogen abstraction to give 3-hydroxy-3-methyl-1-cyclobuten-1-ol and $UO_2(OH)(acac)$. The released 3-hydroxy-3-methyl-1-cyclobuten-1-ol tautomerizes to give the observed product, 3-hydroxy-3-methylcyclobutanone [25]. The remaining uranium species, $UO_2(OH)(acac)$, is unstable, decomposing to produce UO_3 and MeCOCHCOMeH.

4.2. Mechanism of the photolysis of $UO_2(OH_2)(t\text{-Bu–acac})_2$

For the photolysis of $UO_2(OH_2)(t\text{-Bu–acac})_2$ film, FTIR spectroscopy indicated that the reaction was a single-photon process. As the result of the single-photon process, the plot of A_t vs. photolysis time was a single-exponential decay. Both FTIR and Auger electron spectroscopy indicated that UO_3 was the final surface product. The organic products generated from the photolysis were H*t*-BuCOCHCO*t*-Bu, $(CH_3)_3CC(CH_3)_3$, $CH_3COC(CH_3)_3$, $CH_2C(CH_3)COCH_3$ and $(CH_3)_2CHCOCH_3$. These products were observed in MS. Scheme 2 is the proposed mechanism that accounts for all the observations.

The absorption of a photon leads to a ligand-to-metal charge transfer transition involving the transfer of an electron from the donor oxygen on the substituted acac ligand to the uranium. This excitation leads to a diradical species as described above for the case of the simple acac ligand. It is notable that the hydrogen transfer reaction described above is not favorable for this derivative. In this case such a transfer would require a seven-member transition state. Owing to the high energy of such a state an alternate reactivity path dominates. This alternate pathway is more easily visualized using an alternate representation of the electron distribution which is given in Scheme 2. The chemistry is more easily rationalized in this representation. The ligand cleaves to yield a 1-oxo-2,2-dimethylpropyl radical and the uranyl complex [26]. The 1-oxo-2,2-dimethylpropyl radical can eject CO and produce *tert*-butyl a radical [27] which ultimately under-

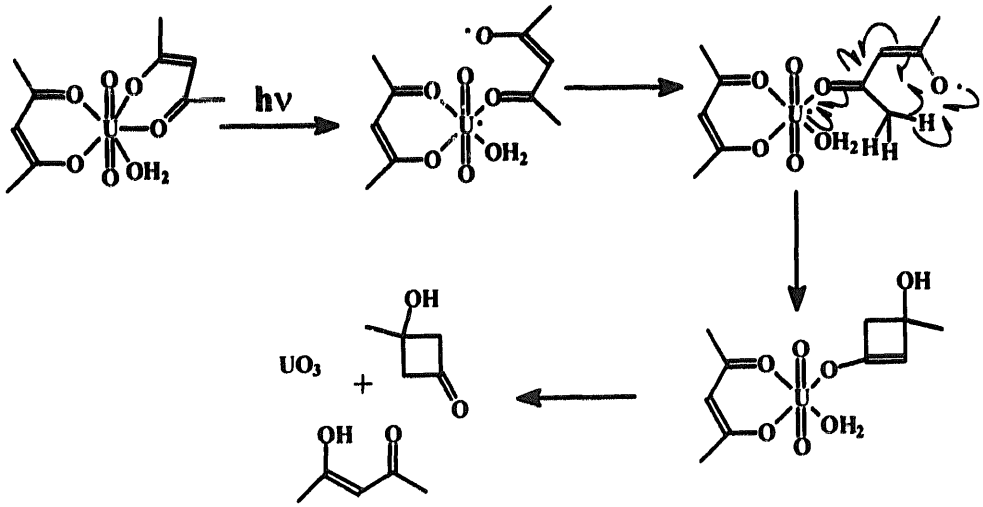

Scheme 1. Proposed mechanism for the photoreaction of a thin film of $UO_2(OH_2)(acac)_2$.

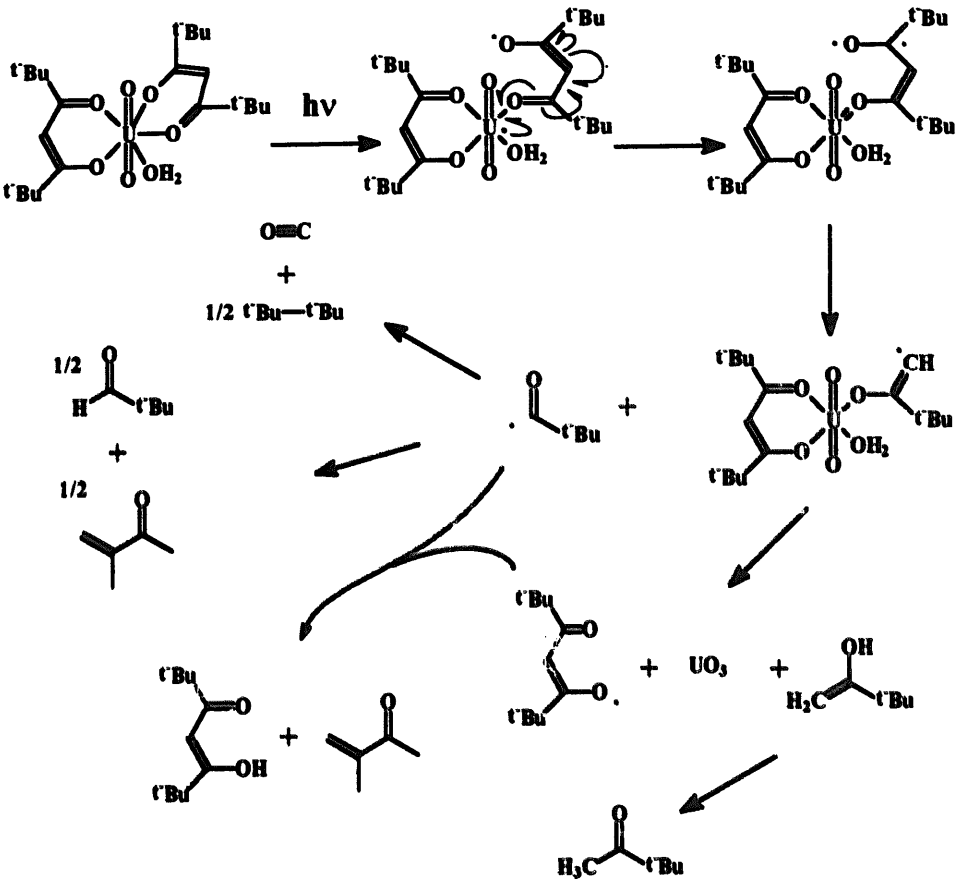

Scheme 2. Proposed mechanism for the photoreaction of a thin film of $UO_2(OH_2)(t\text{-Bu-acac})_2$.

goes combination to yield 2,2,3,3-tetramethylbutane. Alternatively the 1-oxo-2,2-dimethylpropyl radical can disproportionate to yield 2,2-dimethylpropanol and 3-methyl-3-buten-2-one.

The uranyl complex formed has the radical located on the 3,3-dimethyl-1-buten-2-oxy ligand which are the remnants of the cleaved ligand. This complex is unstable and cleaves to yield UO_3, free *tert*-butyl acac radical and 3,3-dimethyl-1-buten-2-ol. This compound tautomerizes to yield the more stable 3,3-dimethyl-2-butanone. The free *tert*-butyl acac ligand can abstract hydrogen from some of the 1-oxo-2,2-dimethylpropyl radical, produced as described above to yield the *tert*-butyl ligand and 3-methyl-3-buten-2-one.

5. Conclusions

The quite distinct products derived from the photolysis of the two 1,3 diketonate complexes may be rationalized to result from the chemistry of the initial photoproduct. In the case of the simple acac ligand the excited state which has an unpaired electron located on the dangling oxygen atom may abstract a hydrogen atom through a six-member transition state. The *t*-Bu–acac derivative does not have this route available to it and as a result a more complicated ligand cleavage route ensues. In each case these initial reactions are occurring in competition with relaxation to the ground state. This result illustrates the danger in comparing the efficiency of photoreactions of even closely related complexes.

Acknowledgment

We thank the Natural Sciences and Engineering Research Council (Canada) for financial support in the form of an operating grant.

References

[1] R.H. Hill, S.L. Blair, C.W. Chu, M. Gao, C.I. Horvath and B.J. Palmer, *Trends Photochem. Photobiol., 3* (1994) 331–341.
[2] S.L. Blair, W. Xia and R.H. Hill, *J. Photochem. Photobiol., A: Chem., 81* (1994) 183–191.
[3] R.H. Hill, A.A. Avey, S.L. Blair, M. Gao and B.J. Palmer, *IUMRS–ICEM '94 Symp. Proc.*, Vol. 1, Materials Research Society, Taiwan, pp. 435–440.
[4] B.J. Palmer and R.H. Hill, *J. Photochem. Photobiol., A: Chem., 72* (1993) 243.
[5] D.G. Bickley, R.H. Hill and C.I. Horvath, *J. Photochem. Photobiol. A: Chem., 67* (1992) 181.
[6] A. Becalska, R.J. Batchelor, F.W.B. Einstein, R.H. Hill and B.J. Palmer, *Inorg. Chem., 31* (1992) 3118.
[7] T.W.H. Ho, S.L. Blair, R.H. Hill and D.G. Bickley, *J. Photochem. Photobiol., A: Chem., 69* (1992) 229.

[8] S.L. Blair, J. Hutchins, R.H. Hill and D.G. Bickley, *J. Mater. Sci., 29* (1994) 2143–2146.
[9] B.J. Palmer, A. Becalska, T.W.H. Ho and R.H. Hill, *J. Mater. Sci., 28* (1993) 6013–6020.
[10] C.W. Chu and R.H. Hill, *IUMRS–ICEM '94 Symp. Proc.*, Vol. 1, Materials Research Society, Taiwan, pp. 441–446.
[11] L.B. Goetting, B.J. Palmer, M. Gao and R.H. Hill, *J. Mater. Sci., 29* (1994) 6147–6151.
[12] I.W. Boyd and R.B. Jackman, *Photochemical Processing of Electronic Materials*, Academic Press, London, 1992, Chapter 4.
[13] R.C. Weast, D.R. Lide, M.J. Astle and W.H. Beyer, *CRC Handbook of Chemistry and Physics*, CRC Press, Boca Raton, FL, 70th edn., p. E. 151.
[14] M.J. Rand, *J. Electrochem. Soc., 120* (1973) 686.
[15] B. Marciniak and G.E. Buono-Core, *J. Photochem. Photobiol., A: Chem., 52* (1990) 1.
[16] A.E. Comyns, B.M. Gatehouse and E. Wait, *J. Chem. Soc.*, (1958) 4655.
[17] L.I. Maissel and R. Glang, *Handbook of Thin Film Technology*, McGraw-Hill, New York, 1970.
[18] A.A. Belyaeva, V.N. Bukhmarina, R.B. Dushin, G.V. Sidorenko and D.N. Suglobov, *Radiokhimiya, 24* (1982) 57.
[19] A. Kiss and J. Csaszar, *Acta Chim. Acad. Sci. Hung., 13* (1957) 49.
[20] H.F. Holtzclaw, Jr., and J.P. Collman, *J. Am. Chem. Soc., 79* (1957) 3318.
[21] R. West and R. Riley, *J. Inorg. Nucl. Chem., 5* (1958) 295.
[22] L. Sacconi and G. Giannoni, *J. Chem. Soc.*, (1954) 2751.
[23] H.R. Hoekstra and S. Siegel, *J. Inorg. Nucl. Chem., 18* (1961) 154.
[24] W. Horspool and D. Armesto, *Organic Photochemistry*, Ellis Horwood, Chichester, West Sussex, 1992, p. 195.
[25] T.H. Lowry, *Mechanism and Theory in Organic Chemistry*, Harper & Row, New York, 2nd edn., 1981, p. 7.
[26] J.K. Kochi, *Free Radicals*, Vol. 1, Wiley, New York, 1973, p. 413.
[27] T.H. Lowry, *Mechanism and Theory in Organic Chemistry*, Harper & Row, New York, 2nd edn., 1981, p. 696.